High Cycle Fatigue Strength of Severely Notched Cast Iron Specimens under Tension and Torsion Loading Conditions

F. Berto[1], P. Lazzarin[1], R. Tovo[2]

[1] University of Padua, Department of Management and Engineering, Stradella San Nicola 3, 36100, Vicenza, Italy
e-mail: berto@gest.unipd.it, plazzarin@gest.unipd.it
[2] University of Ferrara, Department of Engineering, Via Saragat 1, 44100 Ferrara, Italy, email: roberto.tovo@unife.it

ABSTRACT. *The work deals with multi-axial fatigue strength of severely notched cast iron. Circumferentially V-notched specimens were tested under combined tension and torsion loading, both in-phase and out-of-phase, with two nominal load ratios, R=-1 and R=0.The geometry of all axi-symmetric specimens was characterized by a constant notch tip radius (less than 0.1 mm), a notch depth of 4 mm and V-notch opening angle of 90°. The results from multi-axial tests are discussed together with those obtained under pure tension and pure torsion loading from notched specimens with the same geometry. Altogether more than eighty new fatigue data (10 fatigue curves) are summarised in the present work. .*
All fatigue strength data are presented here in terms of the local strain energy density averaged in a specific control volume surrounding the V-notch tip. The dependency of the control volume size as a function of the loading mode is investigated.

INTRODUCTION

Heavy section ductile cast iron components are expected to expand at high rates for the next twenty years. The increased production of wind turbines, or canisters for terminal storage of nuclear waste are an example of this trend. In such applications the use of ductile cast iron is justified by the favourable combination of mechanical (high tensile strength, good wear resistance and ductility) and technological properties (among the ferrous metals, cast irons have the lowest melting temperature and shrinkage and the highest fluidity). The microstructure of ductile cast iron depends on cooling rate, alloying elements, casting temperature and spheroidizing of graphite. The material properties, and in particular the ductility, are influenced above all by the casting microstructure and defects [1, 2]. Even in components cast under optimized conditions, the designer must allow for the presence metallurgical defects, e.g. shrinkage cavities, porosity, slag inclusions and degenerate graphite. Under cyclic loading conditions, such defects tend to behave as cracks. Hence, the endurance of cast components is mainly controlled by the growth of fatigue cracks from casting defects [3-5]. To be able to

determine the size of permissible defects for a given endurance, the designer needs access to reliable fatigue crack growth (FCG) data. For ductile cast iron EN-GJS-400-18-LT, the availability in the open literature of such data is still very limited (see Refs [6-8]), as recently underlined also in Refs [9, 10]. In particular, Zambrano *et al.* [9] studied the fatigue crack growth properties of the ductile cast iron GJS 400. Short, sub-millimetre cracks were observed to grow at a stress intensity range well below the long-crack threshold. Due to the great importance of ductile cast iron GJS-400 in wind turbine design, a further effort has to be made by the researchers to better analyse such short-crack anomalies and, more generally, the fatigue behaviour of this material.

Another important point is that in heavy thick-walled (> 100 mm) components, the desired spherical morphology of the precipitated graphite often degenerates to several different morphologies such as vermicular, spiky, coral, exploded and chunky. In particular, chunky graphite (CHG) is branched and interconnected as a network within eutectic cells and it is observed to form in thermal centres of heavy ductile cast iron sections during solidification [11, 12].

Whereas cracks and internal defects are viewed as unpleasant entities in most engineering materials, U- and V-notches of different acuities are sometimes deliberately introduced in design and manufacturing of products made from cast iron. Moulds, heating elements and chucks are only some examples for industrial components that contain U- or V-shaped notches. A review of literature shows that in spite of some studies on mode I in cracked or plain specimens, there are very few papers focused on multiaxial fatigue behaviour of severely notched cast iron components. A GRP 500/ISO 1083 nodular cast iron was tested in Ref. [13] under torsion loading but considering only plain specimens. In [14] tension and torsion fatigue tests were conducted on unnotched nodular cast iron with quantification of defect size on the fracture surface and the high cycle fatigue reliability was computed by using the Monte Carlo simulation method. A three-parameter Weibull distribution was used in combination with a energy-based and volumetric high-cycle multiaxial fatigue criterion to assess the reliability of the EN-GJS800-2 nodular cast iron [15]. Fatigue failure of a suspension arm made of nodular cast iron was investigated experimentally and a multiaxial criterion was proposed introducing the defect size as input for the criterion [16].

The concept of the curvilinear integral was used to assess some experimental data from cast iron material GTS45 under reversed (alternating) axial and shear stresses both in-phase and out-of-phase and at different frequencies [17].

All the above quoted papers deal with the multiaxial behaviour of smooth notches whereas there is no systematic investigation on the multiaxial fatigue behaviour of severely notched specimens until now. Moreover, it is well known that in the presence of V-shaped notches with a small root radius (ρ=0.1 mm) high cycle fatigue strength is not controlled by the theoretical stress concentration factor K_t. Hence, it is not realistic to estimate the fatigue strength reduction factor K_f on the basis of K_t and the notch sensitivity index. K_f may be estimated from empirical material constants that are adjusted for the agreement with the test data which are provided in the literature for the most commonly used structural steels [18-20] but not for cast iron.

At the light of the observations above, this project is mainly oriented to the definition of a fatigue design methodology for structural components made of EN-GJS400 cast iron and subjected to multiaxial loading conditions in the presence of V-notches with a small root radius (lower than 0.1 mm). The effects of the nominal load ratio, the phase angle and the bi-axiality ratio on the fatigue behaviour are investigated. A final synthesis of the main part of the new data reported in the present work is presented in terms of Strain Energy Density (SED) average over a control volume, which is found to be dependent on on the loading mode, in agreement with previous works dealing with multi-axial fatigue behaviour of steel components [18, 19]

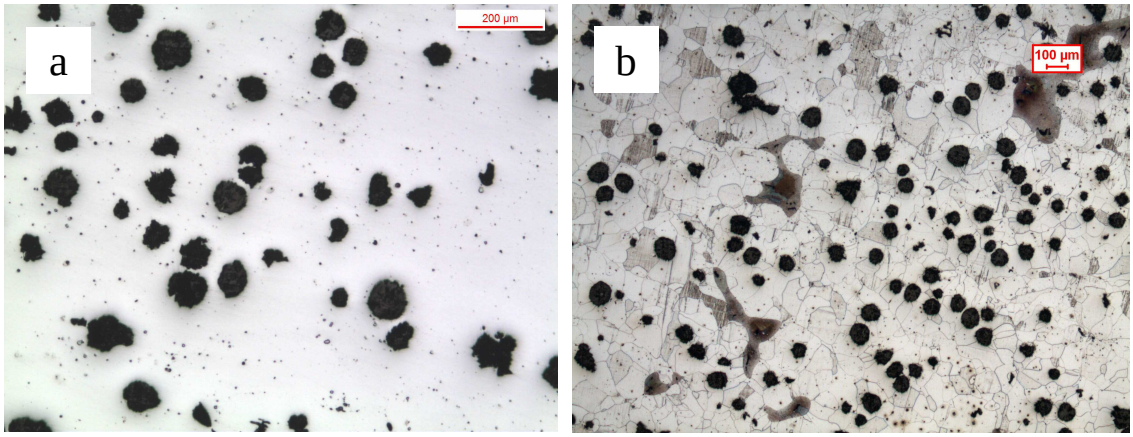

Figure 1. Micrographs of ductile cast iron

MATERIAL AND GEOMETRY OF THE SPECIMENS

All the specimens were made of EN-GJS400 cast iron. The micrographs of the material are shown in Figure 1.
Static tensile tests were carried out to evaluate the elastic and the strength properties of the material. The relevant mean values are listed in Table 1 whereas the chemical composition of the material is reported in Table 2.
The geometry of the specimens tested in the present investigation is shown in Figure 2. The V-notch depth d was equal to 4 mm whereas the notch tip radius, ρ, created by electric discharge machining, was always less than 0.1 mm.
The specimens were tested under pure tension, pure torsion and mixed tension-torsion loading. In particular, 10 different fatigue test series were conducted, according to the following subdivision:

- Two series of tests on V-notched specimens under pure tension and pure torsion fatigue loading at the nominal load ratio R=-1;
- Two series of tests on V-notched specimens under pure tension and pure torsion fatigue loading at the nominal load ratio R=0;
- Four series of tests on V-notched specimens under combined tension and torsion loading, all tested with a biaxiality ratio λ=1; these series were characterised by

two nominal stress ratios, R=0 and R=-1, and by two phase angles, Φ=0, in-phase loading, and Φ=90°, out-of-phase loading;

- Finally, two series of tests on V-notched specimens with the biaxiality ratio λ=0.6 and the nominal load ratio R=-1, both in-phase and out-of-phase.

Table 1. Mechanical properties of the analysed cast iron.

Ultimate tensile strength (MPa)	Yield stress (MPa)	Elongation to fracture (%)
378	267	11.5

Table 2. Chemical composition wt.%, balance Fe.

C	Si	S	P	Mn	Ni	Cr	Mo	V	Cu	Ti	Al	Sb	Mg	Zn
3.50	2.45	0.007	0.020	0.12	0.03	0.04	0.01	0.01	0.13	0.015	0.01	0.001	0.055	0.02

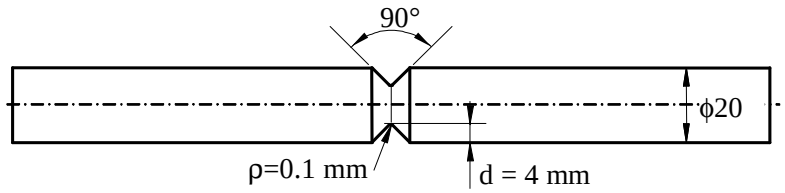

Figure 2: Geometry of the V-notched specimens

FATIGUE TEST DATA FROM V-NOTCHED SPECIMENS

Before being tested, all specimens have been polished in order to both eliminate surface scratches or machining marks and to make the observation of the fatigue crack path easier. Fatigue tests have been carried out on a MTS 809 servo-hydraulic biaxial machine with a 100 kN axial load cell and a torsion load cell of 1100 Nm. All tests have been performed under load control, with a frequency ranging from 1 and 10 Hz, as a function of the geometry and load level. At the end of the fatigue tests, the notch root and the fracture surfaces were examined using optical and electronic microscopy.

The results of statistical analyses carried out by assuming a log-normal distribution are summarised in Table 3. The table gives the mean values of the nominal stress amplitudes at different number of cycles, the inverse slope k of the Wöhler curves and the scatter index T, which quantifies the width of the scatterband included between the 10% and 90% probabilities of survival curves. All failures from 10^4 to $5x10^6$ have been processed in the statistical analysis whereas the run-outs were excluded.

Figure 3 shows fatigue data from specimens tested under combined tension and torsion. In the last case the biaxiality ratio (*i.e.* the nominal (maximum) torsion stress to the nominal tensile stress, τ_a/σ_a, both referred to the net transverse area of the specimen) was set equal to 1 and 0.6. Two nominal stress ratios, R=0 and R=-1, were used. The

presence of a knee located at about 10^6 cycles is evident in the tension case. The knee disappears under torsion as well as under combined tension and torsion loads so that fatigue strength data will be given for specific numbers of cycles to failure: $N_A=2x10^6$ and $N_A=5x10^6$.

Table 3. Results from fatigue tests carried out on V-notched specimens under tension, torsion and combined tension and torsion. Mean values, P_s=50%. All stresses, σ and τ, are refererred to the net transverse sectional area of the specimens.

Series code	Load	No Spec.		k	T_σ or T_τ	σ_a or τ_a		
						10^6	2×10^6	5×10^6
1	Tension, R=–1	7	σ	6.22	1.491	100.5	89.9	77.6
2	Torsion, R=–1	9	τ	13.28	1.163	160.0	151.9	141.8
3	Tension, R=0	6	σ	7.02	1.43	63.5	57.6	50.5
4	Torsion, R=0	9	τ	13.79	1.089	115.2	109.6	102.5
5	R=-1, Φ=0, λ=1.0	12	σ	7.63	1.475	81.0	74.0	65.6
6	R=-1, Φ=90°, λ=1.0	13	σ	15.44	1.183	86.4	82.6	77.8
7	R=0, Φ=0, λ=1.0	7	σ	10.39	1.144	60.3	56.4	51.6
8	R=0, Φ=90°, λ=1.0	6	σ	9.95	1.353	57.1	53.3	48.6
9	R=–1, Φ=0, λ=0.6	5	σ	11.57	1.276	105.9	57.6	92.1
			τ	11.57	1.276	63.5	99.7	55.3
10	R=–1, Φ=90°, λ=0.6	4	σ	9.75	1.365	92.2	59.8	78.2
			τ	9.75	1.365	55.3	85.9	46.9

It is evident from Figure 3 and Table 3 that under multiaxial fatigue loading the effect of out-of-phase angle is very limited for this material both at R=-1 and R=0; conversely, strong is the influence of the nominal load ratio R on the fatigue life, and this holds true also under pure torsion. One should also note that, although the behaviour at high cycle fatigue is the same for Φ=0 and Φ=90°, there is an evident change of the inverse slope k for R=-1 whereas the slope does not change when the nominal load ratio is R=0.

A SYNTHESIS IN TERMS OF LINEAR ELASTIC STRAIN ENERGY DENSITY AVERAGED OVER A CONTROL VOLUME

Local strain energy density averaged in a finite size volume surrounding the notch tip is

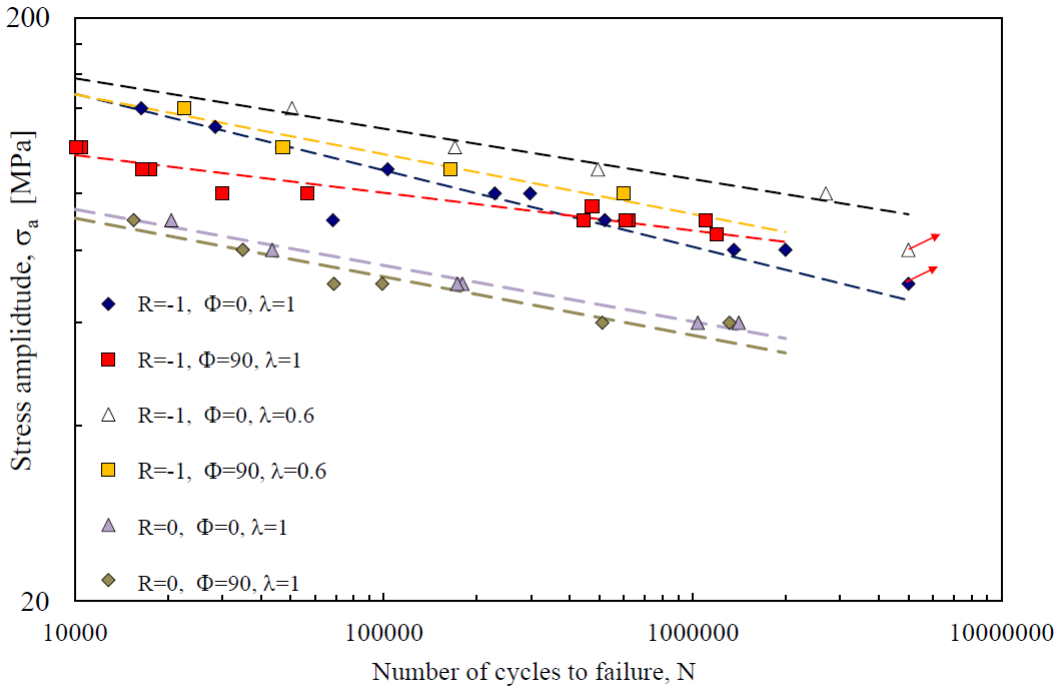

Figure 3: Fatigue data from multiaxial tests

a scalar quantity which can be given as a function of mode I-II NSIFs in plane problems and mode I-II-III NSIFs in three dimensional problems. The evaluation of the local strain energy density needs precise information about the control volume size. In the presence of an axi-symmetric geometry weakened by a circumferential sharp V-notch the averaged SED over a control volume can be expressed under linear elastic hypothesis according to the following relationship:

$$SED = c_W \times \Delta\overline{W} = \frac{1}{E}\left[e_1 \times \frac{\Delta K_1^{\,2}}{R_1^{2(1-\lambda_1)}} + e_3 \times \frac{\Delta K_3^{\,2}}{R_3^{2(1-\lambda_3)}} \right] \quad (1)$$

where ΔK_1 and ΔK_3 are the mode I and Mode III Notch Stress Intensity Factors (NSIFs), R_1 and R_3 are the radiuses of the control volume under Mode I and Mode III loadings, e_1 and e_3 are two parameters that quantifies the influence of all stresses and strains over the control volume [18, 19].

The control volume radiuses R_1 and R_3 can be estimated considering separately the mode I and mode III loadings, by means of the following equations:

$$R_1 = \left(\sqrt{2\, e_1} \times \frac{\Delta K_{1A}}{\Delta \sigma_{1A}} \right)^{\frac{1}{1-\lambda_1}} \quad (2)$$

$$R_3 = \left(\sqrt{\frac{e_3}{1+\nu}} \times \frac{\Delta K_{3A}}{\Delta \tau_{3A}} \right)^{\frac{1}{1-\lambda_3}} \quad (3)$$

In the following, for the sake of simplicity, the stress ranges and the NSIF ranges will be referred at the same number of cycles, $N_A=10^6$. Then, we have:

For mode I loading: ΔK_{1A} = 444 MPa·mm$^{0.455}$; $\Delta\sigma_{1A}$ = 300 MPa.
For mode III loading: ΔK_{3A} = 663 MPa·mm$^{0.333}$; $\Delta\tau_{3A}$ = 292 MPa.

When the opening angle is $2\alpha=90°$, exponents and the parameters assume the following values: λ_1=0.5445, λ_3=0.6667, e_1=0.1462 and e_3=0.3103 (with the Poisson's ratio ν=0.3). As a final result, Eqs (2) and (3) give: R_1=0.63 mm and R_3= 1.37 mm.
In Eq.(1) the coefficient c_W allows us to take into account the influence of the nominal load ratio R. In particular we will use here c_W = 1 for R=0 and c_W = 0.5 for R = −1, as made in previous works dealing with steel notched components.
Figure 4 shows the synthesis based on the local SED. It is evident that a single, quite narrow, scatterband (with T=1.9) is able to summarise all experimental data. The scatter index T would be $\sqrt{1.90}=1.38$ if reconverted in terms of equivalent stress range.

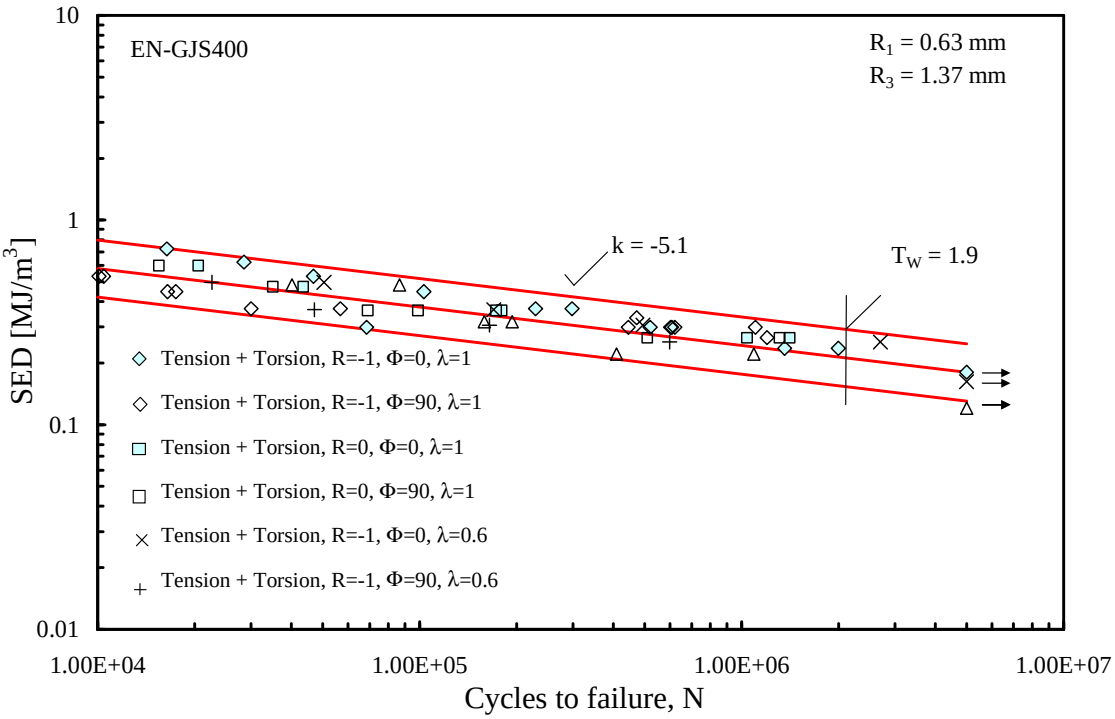

Figure 4. Synthesis in terms of local SED of multiaxial fatigue data

CONCLUSIONS

A large bulk of fatigue data from multi-axial tests on V-notched specimens made of cast iron are discussed together with those obtained under pure tension and pure torsion loading from notched specimens with the same geometry. Altogether more than eighty new fatigue data (10 fatigue curves) are summarised in the present work.

All fatigue strength data from multiaxial tests are presented here in terms of the local strain energy density averaged in a specific control volume surrounding the V-notch tip. The dependency of the control volume size as a function of the loading mode is investigated showing the necessity to introduce two different sizes of the control volume under tension and torsion loadings. The synthesis permits to obtain a quite narrow SED-based scatterband charaterized by a scatter index equal to 1.90.

REFERENCES

[1] Shirani, M., Härkegård, G. (2011) *Eng. Fail. Anal.* **18** ,12-24.

[2] Källbom, R. Hamberg, K. Wessén, M. Björkegren, L.-E. (2005) *Mater. Sci. Eng.* **A413-414** 346-351.

[3] Verdu, C., Adrien, J. and Buffiere, J.Y. (2007) *Mater. Sci. Eng. A* **483–484,** 402-405.

[4] Nadot, Y., Mendez, J. and Ranganathan, N. (2003) *Int. J. Fatigue* **26,** 311-319.

[5] Fjeldstad, A., Wormsen, A. and Härkegård, G. (2007) *Engng. Fract. Mech.* **75**, 1184‑1203.

[6] Hubner, P., Schlosser, H., Pusch, G. and Biermann, H. (2007) *Int. J. Fatigue* **29**, 1788-1796.

[7] Tokaji, K., Ogawa, T. and Shamoto, K. (1994) *Int. J. Fatigue* **16**, 344-350.

[8] Cavallini, M., Di Bartolomeo, O. and Iacoviello, F. (2007) *Engng. Fract. Mech.* **75**, 694-704.

[9] Zambrano, H.R. Härkegård, G. and Stärk, K.F. (2012) *Fatigue Fract. Engng. Mater. Struct.* **35**, 374–388.

[10] Härkegård, G., Svensson, T., Zambrano, H. R. (2012) *Fatigue Fract. Engng. Mater. Struct.* DOI:10.1111/ffe.12008.

[11] Mourujärvi, A., Widell, K., Saukkonen, T. and Hänninen, H. (2009) *Fatigue Fract. Engng. Mater. Struct.* **32**, 379-390.

[12] Ferro, P., Lazzarin, P., Berto, F. (2012) *Mater. Sci. Eng. A* **554**, 122-128.

[13] Marquis, G., Socie, D. (2000) *Fatigue Fract. Engng. Mater. Struct.* **23**, 293–300.

[14] Nasr, A., Bouraoui, Ch., Fathallah, R. and Nadot, Y. (2009) *Fatigue Fract. Engng. Mater. Struct.* **32**, 292–309.

[15] Delahay, T., Palin-Luc, T. (2006) *Int. J. Fatigue* **28**, 474–484.

[16] Nadot, Y., Denier, V. (2004) *Eng. Fail. Anal.* **11**, 485–499.

[17] Stefanov, S.H. (1995) *Int. J. Fatigue* **17**, 567-575.

[18] Berto, F., Lazzarin, P., Yates, J.R. (2011) *Fatigue Fract. Engng. Mater. Struct.* **34**, 921–943.

[19] Berto, F., Lazzarin, P. *Int. J. Fatigue* **33**, 1055-1065.

[20] Tanaka, K., Small Crack Propagation in Multiaxial Notch Fatigue, International Conference on Crack Paths, Gaeta, 19-21 September 2012.